Materials Science Forum *Online: 2007-10-15*
ISSN: 1662-9752, Vols. 558-559, pp 183-188
doi:10.4028/www.scientific.net/MSF.558-559.183

Nucleation mechanism of 40˚<111> rotated grains during recrystallization in heavily cold-rolled Ni_3Al single crystals

Masahiko Demura[1, a], Ya Xu[1,b], Kyosuke Kishida[2,c] and Toshiyuki Hirano[1,d]

[1]Fuel Cell Materials Center, National Institute for Materials Science

1-2-1 Tsukuba, Ibaraki 305-0047, JAPAN

[2]Department of Materials Science and Engineering, Kyoto University

Sakyo-ku, Kyoto 606-8501, JAPAN

[a]DEMURA.Masahiko@nims.go.jp, [b]XU.Ya@nims.go.jp,

[c]k.kishida@materials.mbox.media.kyoto-u.ac.jp, [d]HIRANO.Toshiyuki@nims.go.jp

Keywords: Primary recrystallization, Grain growth, annealing twin, EBSD, Texture.

Abstract. Primary recrystallization textures were examined in the 84% and 95% cold-rolled boron-free Ni_3Al single crystals with a Goss texture using the electron backscatter diffraction method. It was found that the main components of the textures in the specimens heat-treated at 873K/0.5h had a 40˚ rotation relationship about <111> to the original, Goss texture. All the eight variants of 40˚<111> rotated grains existed. However, the number density is not even but dependent on whether the rotation axis is identical to the normal of slip planes activated during the prior cold rolling. The ratio of the number density among the variants was same in both the 84% and 95% cold-rolled foils. Based on these results, the formation of these 40˚<111> rotated grains was explained assuming the modified multiple twinning mechanism where the annealing twinning occurred at the activated slip planes, followed by the subsequent twinning.

Introduction

We have found an interesting texture evolution with heat treatment in heavily cold-rolled Ni_3Al single crystals [1]: disintegration from the cold-rolled texture by primary recrystallization and reintegration into the original, cold-rolled texture by grain growth. This phenomenon can be referred to as texture memory effect. Very recently, it turned out that the texture disintegrated by the primary recrystallization has 40˚ rotation relationship about <111> to the original, cold-rolled texture [2], leading to the assumption that 40˚<111> grain boundary (GB) has a high mobility in Ni_3Al like fcc metals. Based on this assumption, the texture memory effect can be explained as follows. First, in the primary recrystallization, 40˚<111> rotated grains grow preferentially in the deformation because they are surrounded by the 40˚<111> GB. Secondly, during the grain growth, grains with the original, cold-rolled texture, which are surrounded by the 40˚<111> rotated grains, grow preferentially, leading to the reversion to the original, cold-rolled texture. In this explanation, it is, however, not clear how the 40˚<111> rotated grains were formed during the primary recrystallization.

In this study, we examine the microstructures heat-treated at 873K/0.5h, which are considered to keep the characteristics just after the primary recrystallization. Among the characteristics in the microstructure, we focus on the variant selectivity of 40˚<111> rotated grains: the 40˚<111> rotated grains have eight variants which are the crystallographically equivalent to each other, since there are four rotation axis of <111> with two rotation directions. Then, we discuss the formation mechanism of 40˚<111> rotated grains.

Experimental procedures

A Goss-oriented single-crystalline ingot of boron-free Ni-24.0at% Al was grown by the investment casting method. The ingot was cut into two sheets having a thickness of ~2 mm and the two sheets

were cold-rolled to 84% and 95%; the details of the cold rolling were reported in our previous paper [3]. Thus, the two kinds of specimens were prepared in order to clarify the effect of the heterogeneous microstructures such as shear bands; both the specimens exhibit the texture memory effect, as shown in Fig.1. The cold-rolled specimens were heat-treated at 873K for 0.5h in a flowing argon gas after evacuation to a pressure of ~10^{-3}Pa.

The textures were measured on the specimen surface by the X-ray Schultz back reflection method. The orientation maps were determined by the electron backscatter diffraction (EBSD) method in a SEM with a field emission gun with a scanning step of 0.1 μm. The EBSD measurements were performed on the rolling direction (RD) - the transversal direction (TD) sections polished to almost half of the specimen thicknesses.

Results

Cold-rolled specimens. Both of the 84% and 95% cold-rolled specimens exhibit a diffused Goss texture, as shown in Fig. 1 (a) and (d), respectively. The preservation of the {110} texture indicates that the rolling deformation occurred mainly on the two slip planes, (111) and (111,¯) (see the indices in Fig. 1 (a)). There was a spread of the Goss orientation, especially about the normal direction (ND). The extent of the spread becomes larger with the reduction level: it was approximately 20˚ at 84% reduction and larger at 94% reduction.

The 84% cold-rolled specimen exhibited a rather homogeneous microstructure with traces of slip on (111) and (111,¯). According to our previous TEM observations [4], the slip on these two planes occurred without the formation of equiaxed cells or sub-boundaries. In addition, a high density of superlattice intrinsic stacking faults (SISFs) were accumulated on the activated slip planes. No

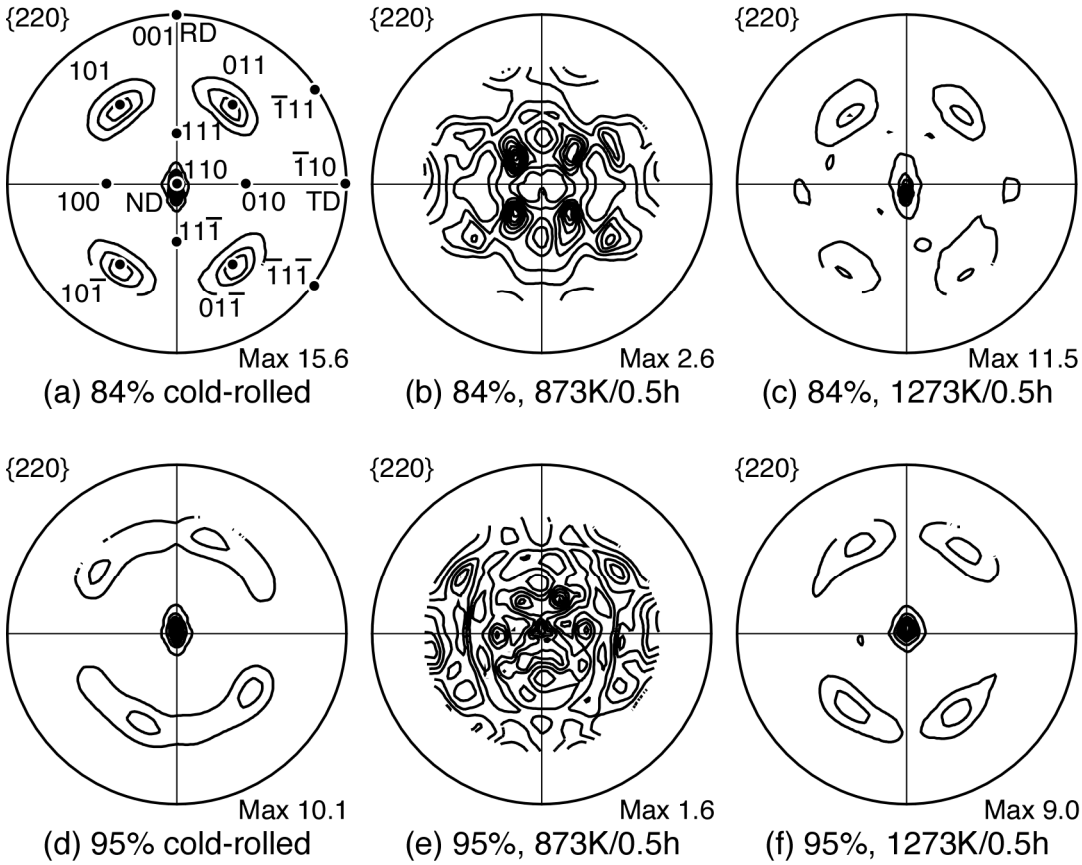

Fig. 1 X-ray{220} pole figures for the cold-rolled and heat-treated Ni_3Al specimens: (a-c) 84% cold reduction; (d-f) 95% cold reduction; (a,d) cold-rolled; (b,c) heat-treated at 873K/0.5h; (c,f) heat-treated at 1273K/0.5h.

Table 1. Average grain size and volume fraction of the Goss, 40˚<111> rotated and other grains in the 84% and 95% cold rolled Ni_3Al specimens that were subsequently heat-treated at 873K/0.5h.

Specimen	Average grain size (μm)	Volume fraction		
		Goss	40˚<111>	Other
84%, 873k/0.5h	0.78	0.06	0.80	0.13
95%, 873k/0.5h	1.03	0.22	0.56	0.23

apparent shear bands were observed. With further cold rolling to 95%, heterogeneities were introduced: deformation bands along RD and shear bands. According to the TEM observation, the shear bands were composed of very fine grains with various orientations [5].

Heat-treated specimens. The maximum intensity of {220} X-ray poles differs between the two specimens (compare Fig. 1 (b) and (e)): it decreases, or becomes closer to that of random distribution, with the increasing cold reduction level. The weaker recrystallization textures in the 95% cold-rolled specimens may originate in its cold-rolled texture (Fig. 1 (d)), which diffused more widely compared to that in the 84% cold-rolled specimen (Fig. 1 (a)).

The SEM observation revealed that the recrystallization completed by the heat treatment at 873K/0.5h in both the specimens. The grain growth occurred more rapidly in 95% cold rolled specimens: the grain size was 0.8 and 1.0 μm in the 84% and 95% cold-rolled specimens, respectively (Table 1). The recrystallization microstructure was characterized by equiaxed grains and a high density of annealing twins. The high density of the annealing twins was confirmed from the EBSD observation: the area fraction of twin boundary reached to over 20% in both the specimens.

Fig. 2 shows the orientation maps where the Goss and the 40˚<111> rotated grains are colored dark and light grey, respectively. Each type of grains was determined with a tolerance of 20˚, considering the orientation spread in the cold-rolled state. Table 1 lists the volume fraction of the Goss and 40˚<111> rotated grains. In the 84% cold-rolled specimen (Fig. 2 (a)), the volume fraction of the Goss grain is very low, and the 40˚<111> rotated grains is dominant. Compared to this, in the 95% cold-rolled specimens (Fig. 2 (b)), there are the Goss grains with a relatively high fraction, though the 40˚<111> rotated grains are still the major component. Remembering that the grain growth occurred more rapidly in the 95% cold-rolled specimens, the relatively high fraction of the Goss grains means that the reversion to the original, Goss texture has started at this heat treatment condition of 873K/0.5h.

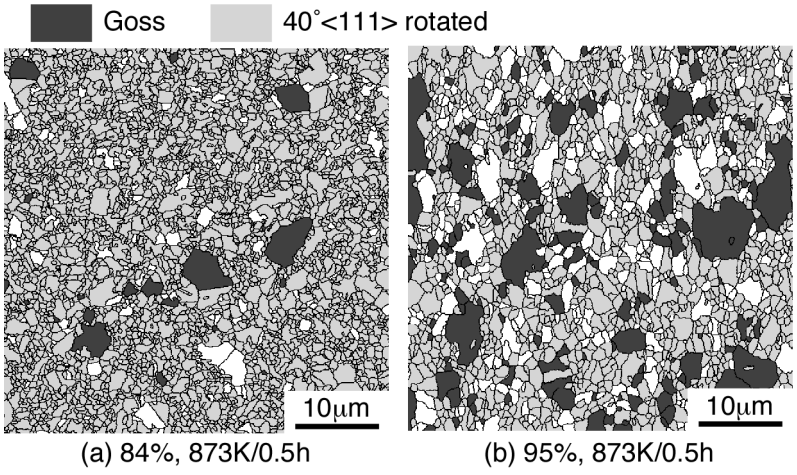

Fig. 2 Orientation maps obtained from the EBSD measurements on the RD-TD sections of the 84% and 95% cold-rolled Ni3Al specimens, both of which were subsequently heat-treated at 873K/0.5h: dark and light grey grains are Goss and 40˚<111> rotated grains, respectively.

Table 2. Volume fraction, number density, and grain size of each variant.

Specimen	Rotation axis of 40˚<111>	Volume fraction	Number density (mm^{-2})	Grain size (μm)	Slip plane normal?
84%, 873k/0.5h	1 1 1 and 1 1 $\bar{1}$	0.07	1.3E+05	0.75	Yes
	$\bar{1}$ 1 1 and 1	0.13	2.2E+05	0.74	No
95%, 873k/0.5h	1 1 1 and 1 1 $\bar{1}$	0.05	5.0E+04	1.03	Yes
	$\bar{1}$ 1 1 and 1	0.09	9.2E+04	0.97	No

Regarding the variant selectivity of the 40˚<111> rotated grains, we determined the volume fraction, number density, and the size of each variant. All the eight variants existed and their sizes were almost the same between each other. However, the volume fraction and the number density were not even but dependent on whether the rotation axis is identical to the normal of the activated slip planes, (111) and ($\bar{1}$11). According to this dependency, Table 2 summarizes the volume fraction, number density and size. The volume fraction and number density of the variants rotated about the normal of the activated slip planes are almost a half of those of the other variants. It is noted that this ratio is almost the same irrespectively of the prior cold reduction level, though the values of the volume fraction and number density are different corresponding to the progress of grain growth.

Discussion

The 84% cold-rolled specimen had a very high volume fraction of the 40˚<111> rotated grains, 80%, after the heat treatment at 873K/0.5h, and thus the obtained results can be assumed to keep characteristics just after the primary recrystallization. In the case of the 95% cold-rolled specimen, grain growth proceeded and the volume fraction of the 40˚<111> rotated grains descended due to the preferential growth of the Goss grains. Nevertheless, it can be assumed that the variant selectivity, i.e. the number density ratio among variants, is the same as that just after the primary recrystallization. This is because there was no difference in growth rate among the variants. Consequently, the variant selectivity obtained by the heat treatment of 873K/0.5h (Table 2) can be regarded as the ratio of the formation frequency among the variants during the primary recrystallization in both of the 84% and 95% cold-rolled specimens.

The 84% cold-rolled specimen exhibited a homogeneous microstructure with a Goss texture. With further cold rolling to 95% reduction, orientation spread became wider and shear bands developed. The shear bands are known to be the places where recrystallization takes place preferentially, and in heavily cold-rolled Ni_3Al the preferential nucleation at the shear bands was reported [6,7]. As mentioned in Results, the shear bands in the heavily cold-rolled Ni_3Al were composed of very fine grains with various orientations [5]. Thus, there may be 40˚<111> rotated grains in the shear bands. They are, however, considered to have a negligibly small effect because the variant selectivity of the 95% cold-rolled specimen is the same as that of the 84% cold-rolled one where shear bands was not observed macroscopically. In other words, it is necessary to assume that the 40˚<111> rotated grains were formed in the homogeneous deformation microstructure.

In the recrystallization microstructure, a high fraction of annealing twins were observed. If annealing twining occurs many times successively, a broad variety of new orientations appear. This process is referred to as multiple twinning mechanism and examined so far by calculation [8,9] and TEM observation [10] in fcc metals.

Table 3. Number of sequences of multiple twinning which yield the 40°<111> rotated orientations. The 12 sequences are listed assuming that the first annealing twinning occurs on the activated slip planes, (111) and (111,¯).

Variants		Number of sequences	Slip plane normal?
Rotation axis	Rotation angle		
[1 1 1]	40	1	Yes
[1 1 1]	-40	1	Yes
[1 1 1,¯]	40	1	Yes
[1 1 1,¯]	-40	1	Yes
[1,¯ 1 1]	40	2	No
[1,¯ 1 1]	-40	2	No
[1 1,¯ 1]	40	2	No
[1 1,¯ 1]	-40	2	No

Based on the multiple twinning mechanism, the authors have recently proposed the idea to explain the formation of the 40°<111> rotated grains, as follows [2]. In Ni_3Al having the fcc-based $L1_2$ structure, there are four equivalent twinning planes of {111} similarly to fcc metals. According to calculation, there are 24 sequences which yield the orientations close to the 40°<111> rotated orientations in the 6th generation multiple twinning, where twinning occurs six times: the misorientation was 2.7° between the orientations generated by these 24 sequences and the exact 40°<111> rotated orientations.

The 24 sequences bring about all the eight variant and it was found that if the 24 sequences occur with equal probability, there should be no variant selectivity. In fact, however, the variant selectivity was observed depending on whether the rotation axis is the normal of the activated slip planes. In order to explain this variant selectivity, we assume that the prior slip deformation accelerates the twinning process on the activated slip planes, (111) and (111,¯). This assumption seems to be reasonable, remembering that there are a high density of SISFs on the activated slip planes. The SISFs are likely to yield a flawed {111} stacking during the grain boundary movement, which is believed to be the cause of annealing twinning [11]. This acceleration mechanism by the SISFs can work only on the first annealing twinning whose twinning planes are identical to the {111} planes in the original, Goss orientation.

As an extreme case, let us consider that the first annealing twinning occurs only on the activated slip planes and that the subsequent and higher generation twinning occurs on all the {111} planes with equal probability. According to this assumption, 12 sequences are chosen and the number of the sequences for each variant is summarized in Table 3. The total number of the sequences for the variants rotated about the normal of the activated slip planes is just the half of that of the others. This number ratio is in fairly good agreement with the observed variant selectivity. Thus, in the heavily cold-rolled Ni_3Al single crystals, the multiple twinning mechanism can explain the difference in the formation frequency among the eight variants.

Conclusions

The textures after the heat treatment at 873K/0.5h was examined in the 84% and 95% cold-rolled single crystals with a Goss texture, and the following results were obtained:

1. The 84% cold-rolled foils had a homogeneous microstructure where the two slip planes, (111) and (111,¯), were activated. With the further cold rolling to 95%, the heterogeneity such as shear bands was introduced.
2. The recrystallization completed at 873K/0.5h and a high density of annealing twins were observed.
3. The main components of the textures in the specimens heat-treated at 873K/0.5h were 40˚<111> rotated grains.
4. All eight variants of the 40˚<111> rotated grains were observed and the size is almost the same among them.
5. There was a variant selectivity, as follows: the number density and the volume fraction of the variants having a rotation axis identical to the normal of the activated slip planes is almost a half of those of the other variants.
6. There was no difference in the variant selectivity between the 84% and 95% cold-rolled specimens, showing that the effect of the shear bands was negligibly small.
7. The above features can be explained assuming that the 40˚<111> rotated grains were formed from the original, Goss texture by multiple twinning mechanism where the first annealing twinning was assumed to occur on the activated slip planes.

Acknowledgements

The authors would like to thank M. Takanashi for his helpful assistance in the sample preparation. This work was partly supported by a Grant-in-Aid for Young Scientists (B) (No. 18760536) from the Ministry of Education, Culture, Sports, Science and Technology (MEXT).

References

[1] M. Demura, K. Kishida, Y. Xu and T. Hirano: Mater. Sci. Forum Vol. 467–470 (2004), p. 447.

[2] M. Demura, Y. Xu, K. Kishida and T. Hirano: Acta mater. (2006), in press.

[3] M. Demura, Y. Suga, O. Umezawa, K. Kishida, E.P. George and T. Hirano: Intermetallics Vol. 9 (2001), p. 157.

[4] K. Kishida, M. Demura and T. Hirano, in: Proceedings of the Materials Research Society Symposium, edited by M.J. Mills, H. Inui, H. Clemens and C.-L. Fu, Materials Research Society, Boston, MA, (2005), p. S5.22.1.

[5] K. Kishida, M. Demura, S. Kobayashi, Y. Xu and T. Hirano: Defect and Diffusion Forum Vol. 233–234 (2004), p. 37.

[6] C. Escher and G. Gottstein: Acta mater. Vol. 46 (1998), p. 525.

[7] S. Zaefferer: Mater. Sci. Forum Vol. 495–497 (2005), p. 3.

[8] C.M.F. Rae, C.R.M. Grovenor and K.M. Knowles: Z. Metallkde. Vol. 72 (1981), p. 798.

[9] G. Gottstein: Acta metall. Vol. 32 (1984), p. 1117.

[10] P. Haasen: Metall. Trans. A Vol. 24A (1993), p. 1001.

[11] S. Mahajan, C.S. Pande, M.A. Imam and B.B. Rath: Acta mater. Vol. 45 (1997), p. 2633.